JOURNAL OF AGRICULTURAL AND FOOD CHEMISTRY

Phase Transitions, Solubility, and Crystallization Kinetics of Phytosterols and Phytosterol−Oil Blends

HARIKLIA VAIKOUSI,† ATHINA LAZARIDOU,† COSTAS G. BILIADERIS,*,† AND JERZY ZAWISTOWSKI‡

Laboratory of Food Chemistry and Biochemistry, Department of Food Science and Technology, School of Agriculture, Aristotle University, Thessaloniki, Greece, and Forbes Medi-Tech, Vancouver, British Columbia, Canada

The thermal properties, solubility characteristics, and crystallization kinetics of four commercial phytosterol preparations (soy and wood sterols and stanols) and their blends with corn oil were examined. Differential scanning calorimetry (DSC) revealed narrow melting peaks between 138 and 145 °C for all phytosterol samples, reversible on rescan. Broader and less symmetrical melting transitions at lower temperatures with increasing oil content were observed for two samples of phytosterol−oil admixtures. The estimated, from the solubility law, ΔH values (34.7 and 70.7 mJ/mg for wood sterols and stanols, respectively), were similar to the DSC experimental data. Fatty acid esters of soy stanols differing in the chain length of the acyl groups (C2−C12) exhibited suppression of the melting point and increase of the fusion enthalpy with increasing chain length of the acyl group; the propionate ester exhibited the highest melting point (T_m: 151 °C) among all stanol−fatty acid esters. Solubility of phytosterols in corn oil was low (2−3% w/w at 25 °C) and increased slightly with a temperature rise. Plant sterols appeared more soluble than stanols with higher critical concentrations at saturation. The induction time for recrystallization of sterol−oil liquid blends, as determined by spectrophotometry, depended on the supersaturation ratio. The calculated interfacial free energies between crystalline sediments and oil were smaller for sterol samples (3.80 and 3.85 mJ/m^2) than stanol mixtures (5.95 and 6.07 mJ/m^2), in accord with the higher solubility of the sterol crystals in corn oil. The XRD patterns and light microscopy revealed some differences in the characteristics among the native and recrystallized in oil phytosterol preparations.

KEYWORDS: Phytosterols; DSC; thermal transitions; solubility; crystallization; surface free energy; XRD; microscopy

INTRODUCTION

Plant sterols (phytosterols) have generated interest in the functional food industry as they have been shown to reduce the levels of serum low-density lipoprotein (LDL) cholesterol in humans. A meta-analysis of over 40 clinical trials showed that an intake of 2 g/day of stanols or sterols reduced LDL cholesterol by ca. 10% (*1*). These compounds are structurally similar and functionally analogous to cholesterol in animals (*2*). Phytosterols are naturally found in foods of plant origin, principally oils, but also in seeds (e.g., pulses), dried fruit, bread, and cereals (*3*). Another important source of phytosterols is tall-oil, the fat soluble fraction of the hydrolysate obtained from trees during the pulping process (*4*).

Since phytosterols are not synthesized in the human body, they must be supplied via one's diet (*2*). Whereas about 50% of cholesterol is absorbed in the intestinal tract, plant stanols and sterols are absorbed at a lower extent; absorption is about 10−15% for campesterol and campestanol, 3−5% for sitosterol and stigmasterol (*5*−*7*), and 1% for sitostanol (*8*). Phytosterols have been applied for the lowering of blood cholesterol for almost five decades, and it is a commonly accepted viewpoint that the decrease of blood cholesterol induced by phytosterols is due to their interference with the intestinal absorption of both dietary and biliary cholesterol and, consequently, enhancement in fecal excretion of cholesterol (*3*).

Many studies have been conducted on the hypocholesterolaemic effects of phytosterol-enriched foods in humans, and well-documented reviews summarize the data from published clinical trials (*1*, *2*, *9*, *4*, *10*, *11*). In early studies on the cholesterol-lowering efficacy of plant sterols, the sterols were in the crystalline, unesterified (or free) form, and high daily intakes (5−10 g) were necessary to achieve significant lowering of cholesterol (*12*). The effectiveness of plant sterols is highly dependent on their physical state. To be able to compete with cholesterol for solubilization in the mixed micelles of the

* Corresponding author. Phone: +30-2310991797 and +30-2310471467. Fax: +30-2310471257. E-mail: biliader@agro.auth.gr.
† Aristotle University.
‡ Forbes Medi-Tech.

10.1021/jf0624289 CCC: $37.00
Published on Web 02/13/2007

Table 1. Source, Purity, and Composition of Phytosterol and Phytostanol Samples

sample ID	compound	soy stanols (SSN)	soy sterols (SST)	wood sterols–stanols (WSTSN)	wood stanols (WSN)
total sterol content (% w/w)[a]		99.8	86.2	99.6[b]	89.2[c]
major phytosterols (% w/w)[a]	sitostanol	62.3[c]		20.8[c]	79.6[c]
	campestanol	36.3[c]		2.7[c]	9.7[c]
	sitosterol		36.8[d]	60.3[c]	
	campesterol		23.5[d]	6.9[c]	
	stigmasterol		23.1[d]		
	brassicasterol		2.8[d]		
minor phytosterols (% w/w)[a]	total minor phytosterols	1.2[b]		8.9[b]	

[a] On anhydrous basis. [b] GCMS, manufacturer's specification. [c] GC/FID, manufacturer's specification. [d] GC, manufacturer's specification.

intestine, plant sterols should be evenly distributed in the intestinal contents and have a high effective surface area in the carrier vesicles (*13*). The maximum effectiveness of plant sterols can be obtained only if they are present in the intestine simultaneously with the cholesterol. The preferred carrier would be dietary fat as for dietary cholesterol (*14*). Enrichment of food products with plant sterols is difficult from a technological and food quality point of view since they are insoluble in water and poorly soluble in dietary fats. Both the sensorial properties and cholesterol-lowering efficacy may thus be compromised (*12*). Consequently, much effort has been placed on finding approaches that overcome these limitations. Esterification of the plant sterols and stanols with unsaturated fatty acids increases their lipid solubility (approximately 10-fold) and thus facilitates their incorporation into fat containing foods. Two or three grams per day of esterified phytosterols are necessary to achieve a sufficient serum cholesterol reduction of 10%, while most probably, the same effect can be attained with an even smaller amount of non-esterified phytosterols (*15*). Margarines and table spreads are ideal vehicles for these bioactives, although cream cheese, salad dressings, and yogurts are also used as delivery systems. On the other hand, the incorporation of phytosterols in a liquid oil medium produces relatively unstable systems that may develop turbidity during storage due to sterol recrystallization and precipitation of the previously dissolved crystalline material.

Phytosterol crystallization in oil-based media is an undesirable phenomenon that affects the product's shelf life and the final product acceptability from a consumer's point of view. Crystal nucleation is a prerequisite for crystallization and the consequence of the metastable state that occurs after supersaturation. Supersaturation can be achieved by removing solvents, by cooling, or by adding a precipitant, and it may also be the result of a chemical reaction (*16*). Once the nuclei have formed, they grow and develop into crystals (*17*). Crystallization is sensitive to the extent of supersaturation, temperature, as well as the presence of impurities. Crystal growth can occur by a variety of mechanisms according to the conditions occurring during crystallization and the substance being crystallized. The growth rate of the crystals depends on their particle size, the viscosity of the dispersion, the presence of impurities, and the application of agitation in the cooling solution (*18*). However, supersaturated oil may remain remarkably stable for a period of time that depends on several factors, including the extent of supersaturation, temperature, and the surface free energy between solute and oil. To our knowledge, no previous studies have dealt with crystallization kinetics and the stability of phytosterols in edible oils.

The purpose of the present work was to investigate the thermal properties and phase transition behavior of four phytosterol samples (commercial sterols and stanols) from different plant sources (soy or wood derived) and their blends with corn oil. The solubility characteristics and the stability of phytosterol solutions in corn oil with respect to crystallization kinetics, as well as the crystal structure/habit, are all useful information in assessing the potential of oil-based delivery systems for phytosterols as functional ingredients in food products.

MATERIALS AND METHODS

Materials. Phytosterol and/or phytostanol samples were kindly offered by Forbes Medi-Tech Inc. (Vancouver, Canada). The plant source (soy or wood), purity, and composition of four industrial preparations are presented in **Table 1**. The GC/FID and GCMS analyses for the identification and quantification of the major and minor sterol and stanol components of the samples were conducted by Forbes Medi-Tech Inc. Sterols derived from soy (SST) and its hydrogenated product (soy stanols, SSN) and a mixture of wood sterols and stanols (WSTSN) and its hydrogenated derivative of wood stanols (WSN) were the four preparations used in this study. Fatty acid esters of soy stanols (SSN) differing in the chain length of the acyl group (C2−C12) were also obtained from the same plant sterol manufacturer. Corn oil (Flora, Elais) was purchased from the local market and used for preparation of all phytosterol−oil liquid blends or admixtures. Acetone (analytical grade) was obtained by Riedel-de Häen (Seelze, Germany).

Differential Scanning Calorimetry (DSC). The phase transition behavior of the native phytosterol mixtures was probed by differential scanning calorimetry, using a PL DSC−gold calorimeter (Polymer Labs. Ltd, Epsom, UK). Heat flow calibration was made by reference to the known melting enthalpy of indium (purity 99.99%), whereas temperature calibration was made with cyclohexane, dodecane, and octane. Samples of about 4−6 mg (previously stored in the freezer, −18 °C) were sealed hermetically into DSC pans and heated from 20 to 180 °C under continuous flow of dry N_2 gas at a heating rate of 5 °C/min with an empty pan as an inert reference. Slow cooling and rescanning of samples under the same heating rate was also made. To investigate the melting behavior of phytosterols in a corn oil liquid medium, samples were prepared by mixing specified amounts of dry sterol powders (samples of WSTSN and WSN preheated at 110 °C for 40 min and cooled at room temperature over silica gel) with appropriate portions of corn oil to obtain phytosterol−oil admixtures of different weight ratios of the two components. The peak melting temperature of the crystals was taken as the temperature of the DSC main peaks. All DSC experiments were conducted at least in triplicate, while the given DSC thermograms were normalized on a constant weight basis of crystal solids.

Dispersion−Solubilization of Phytosterol−Oil Blends. Samples of phytosterol and phytostanol mixtures stored in the freezer (−18 °C) were preheated at 110 °C for 40 min and subsequently cooled in a desiccator over silica gel at ambient temperature for the removal of the moisture present. Dispersions of phytosterols−phytostanols in oil of varying concentrations were prepared by mixing a known amount of the dry powdered crystals in corn oil on a weight-to-weight basis (mass of sterols per mass of oil, w/w) in screw capped test tubes under stirring. Suspensions were then heated at 80−90 °C until complete solubilization and melting of crystals and then allowed to cool at 25 °C for further observation and analysis. Depending on the phytosterol

type and concentration, newly formed crystals eventually appeared in the clear oil medium, implying recrystallization of the plant sterol components.

Solubility of Phytosterol in Corn Oil. Determination of the approximate solubilities of sterol/stanol samples in corn oil at different temperatures was performed as follows: a series of solutions of all phytosterol samples in the concentration range from 1 to 10% w/w, with an incremental step of 1%, was prepared for each sterol−oil combination in 20 mL glass test tubes with caps containing magnetic stirrers. The tubes were heated up to 85 °C in a water bath, and after complete dissolution of the crystalline material, the bath temperature was set to the desired observation temperature (50, 45, 40, 35, 30, and 25 °C), and solutions were allowed to cool slowly under gentle stirring. Agitation is generally necessary to bring liquid and solid phases into intimate contact and facilitate equilibration. Prolonged contact with agitation is required between excess solid solute and liquid phase at a constant temperature, usually for several hours (*16*). The solubility limits at different constant temperatures after 24 h stirring were evaluated visually by registering the formation of crystals. Tubes with no presence of crystalline phase or cloudiness were characterized as clear solutions.

Determination of the Concentration at Saturation (C_s) for Crystallization to Begin. For nucleation, the achievement of supersaturation or supercooling is necessary by reaching a concentration of the solute, C, higher than the concentration at saturation, C_s. Once the nuclei have formed, they grow and develop into crystals (*18*).

Since the solubility data for phytosterol samples were known approximately, the preparation of a phytosterol−oil solution with a concentration slightly higher than that observed by the solubility data at the specific temperature would result in supersaturation of the system and subsequently the formation of the first nuclei leading to crystallization. The yield of the formed crystals, if collected and adequately separated from the oil medium, represents the excess portion of solute that could not be dissolved in oil, at the given temperature, and thus precipitated as sediment. Thus, with the initial solution concentration known, the gravimetric difference between the initial amount of sterols dissolved and the mass of the obtained crystals would give the mass of sterols present at equilibrium, or in other words, the concentration at saturation. Phytosterol−oil liquid blends were prepared at concentrations of 3 and 4% w/w for each sample (in triplicates) as described previously, and crystallization was allowed to occur at 25 °C. The test tubes were not agitated during the cooling step of the treatment, but solutions were held for a period of 72 h, so crystallization was completed slowly and naturally. The crystals formed were collected by carefully filtering the oil suspensions under vacuum through a dried (preheated at 110 °C for 2 h) and preweighed paper filter. The filter was washed thoroughly 3 times with cold acetone for the removal of any residual oil (mother liquor) retained by the crystals, dried overnight in a vacuum drying oven at ambient temperature, and finally weighed for the gravimetric determination of the concentration at saturation.

Spectrophotometric Kinetic Study of Phytosterol Crystallization. Crystallization kinetics was studied isothermally at 25 °C by following the change of transmitted light through the oil samples during the course of clouding using a spectrophotometer (SP-8001 UV−vis, Metertech Inc., Taipei, Taiwan). Supersaturated sterol−oil solutions in screw capped test tubes (with different supersaturation rates) were first heated at 80 °C for 30 min to melt all crystals and slowly cooled before being transferred into a quartz cuvette (at about 30 °C). When the temperature reached 25 °C, the time course of changes in transmittance values at 600 nm was recorded. At this temperature, the sterol−oil mixture initially appeared clear, and it eventually developed turbidity as nucleation occurred and crystals began to grow. The period of time that usually elapses between the achievement of supersaturation and the appearance of crystals (turbidity development in this case) is generally referred to as the induction time or latent period (*16*) and can be determined graphically from the transmittance−time curve (*19*). The coefficients of variation for repeated measurements of induction times (time to reach $T < 97\%$) did not exceed 12% in all cases. Crystallization kinetics was performed at least in triplicate for each phytosterol−oil blend tested to take an average induction time value for the determination of the interfacial free energy between phytosterol crystals and corn oil, as will be discussed later.

X-ray Diffraction and Microscopy. X-ray diffraction (XRD) was used to analyze the crystal structure of phytosterol samples. Three types of crystals were examined: (a) native phytosterol crystals in the powder form (samples from the freezer that were previously dehydrated at 110 °C for 40 min), (b) crystals isolated after their recrystallization in phytosterol−oil liquid mixtures (at a concentration of 4% w/w) at 25 °C in test tubes without agitation, and (c) crystals obtained from recrystallized sterol−oil mixtures at the same concentration under gentle agitation during the cooling step of the treatment and crystal formation. Crystals in cases b and c were collected after filtration and washing with cold acetone, as described previously. Crystalline specimens were subjected to WAXRD analysis at 25 °C using a Philips diffractometer (PW 1830 generator, equipped with a graphite-crystal monochromator and a vertical PW 1830 goniometer). The operating conditions were Cu Kα radiation ($\lambda = 0.15418$ nm) in reflection mode, voltage 40 kV, amperage 30 mA, sampling interval time 0.4 s, and a diffraction angle (2θ) range from 7 to 40° (step size 0.05°). The morphological features of the phytosterol crystal types described previously were evaluated using light microscopy. Microphotographs of crystals were taken using an Olympus BX61 light microscope equipped with dry lenses and an Olympus DP70 color digital camera attached to the microscope. Small amounts of the collected crystals were suspended in corn oil and visually observed for differences in shape and size.

RESULTS AND DISCUSSION

Thermal Behavior of Phytosterol−Phytostanol Crystals. Representative DSC thermal curves for melting of the plant sterol preparations are shown in **Figure 1**. All phytosterol samples exhibited narrow melting endotherms between 138.18 ± 0.27 and 144.56 ± 0.35 °C, fully reversible on rescan. The main single DSC melting peak indicates that all components in each phytosterol mixture have similar melting properties and crystal forms. Furthermore, smaller and broader endothermic transitions at lower temperatures (97−105 °C) were also observed for all samples, which disappeared in almost all cases after cooling and immediate reheating of the samples (curves assigned letter b). After the first melting and release of moisture, the materials crystallized into their original form, showing sharp melting transitions (T_m between 138 and 144 °C). However, for wood stanols (WSN), the broad low-temperature endotherm was present even in the rescan, implying the coexistence of a different crystal type that melts at a lower temperature. A DSC analysis study conducted by Narayana Kalkura and Devanarayanan (*20*), on β-sitosterol crystals grown in silica gel, also revealed two endothermic peaks at 100 and 140 °C that were attributed to the loss of hydration water and to the melting of the crystals, respectively. In addition, two wide endothermic peaks below the original melting peak were shown in the thermogram of β-sitosterol precipitated from an acetone−water mixture, which corresponded to the dehydration of β-sitosterol monohydrate occurring in two separate stages; first, half of the hydration water leaves the crystal and a hemihydrate crystal is formed (below 60 °C), while at the second dehydration stage, the rest of the hydration water leaves the crystal below 90 °C (*13*, *21*). The plant origin as well as the chemical composition (sterols vs stanols) did not seem to largely affect the phase transition behavior of the isolated sterol mixtures since all samples exhibited endotherms in the same temperature region. Similar melting peaks were observed at 138.1 ± 0.6 °C for pure β-sitosterol recrystallized from acetone by Christiansen et al. (*21*) and at 133.1 and 141.3 °C for sitosterol and sitostanol, respectively, by Melñikov et al. (*3*). The average melting enthalpies for SSN, SST, WSTSN, and WSN, as determined from the DSC peak areas of the rescans, were 45.6 ± 2.1, 39.5 ± 1.2, 39.08 ± 1.74, and 74.9 ± 2.18 mJ/mg (the latter being the sum of the two endothermic transitions observed for

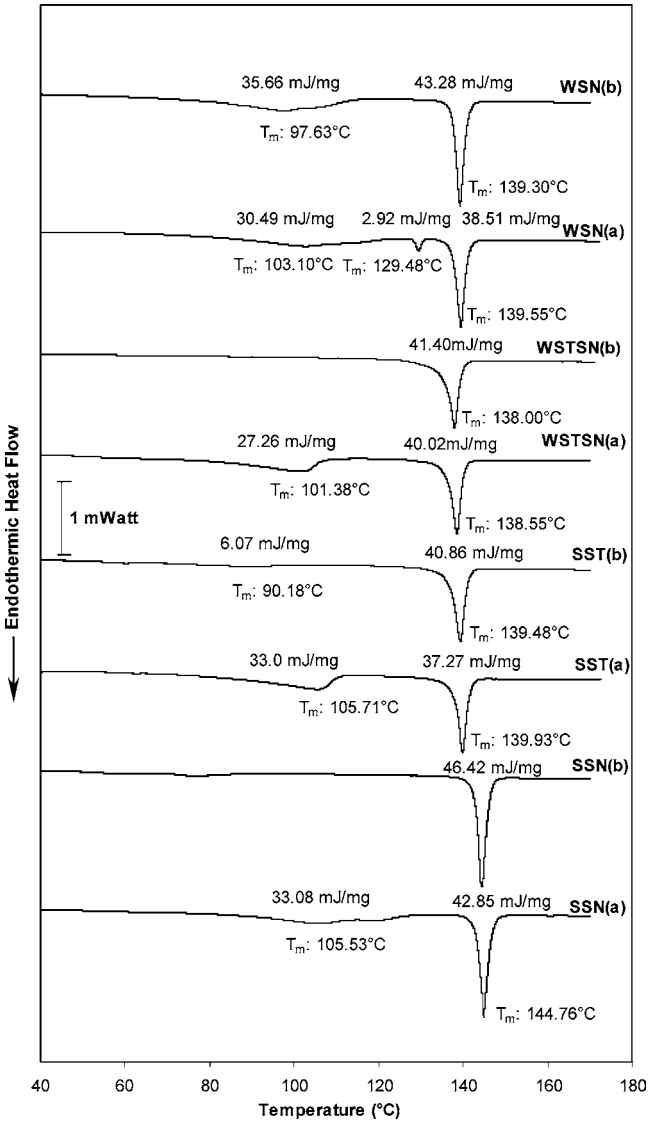

Figure 1. DSC thermograms of native (**a**) and after the rescan (**b**) phytosterol samples; heating rate 5 °C/min, sample identification in abbreviated form as specified in **Table 1**.

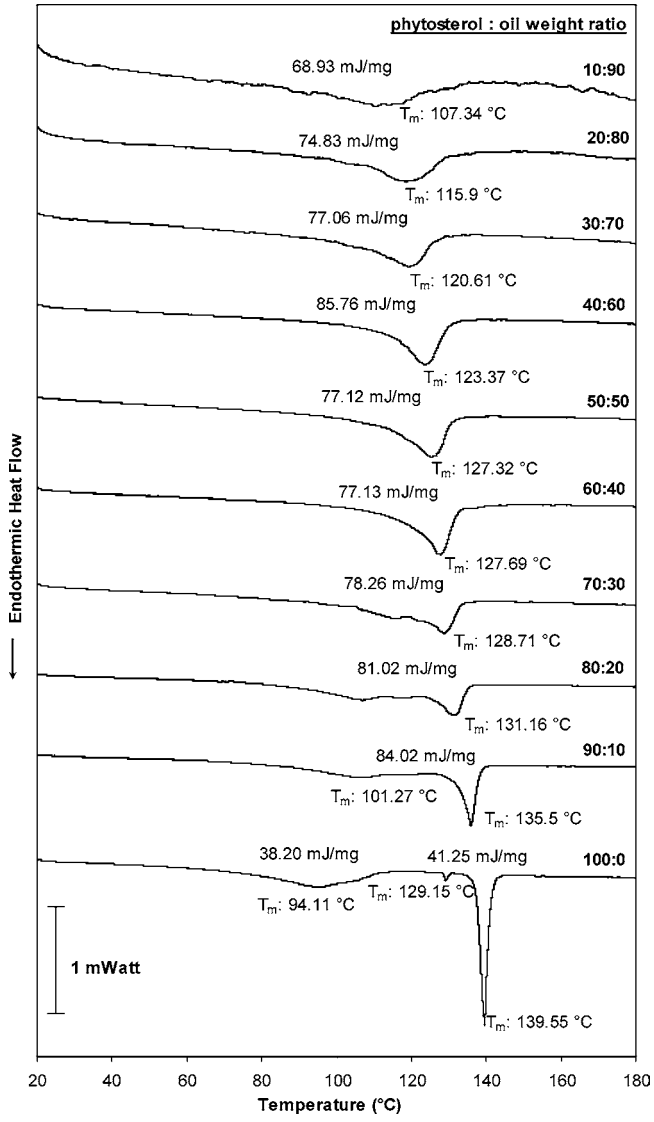

Figure 2. DSC melting traces of wood stanol, WSN (preheated at 110 °C for 40 min)–corn oil mixtures at varying weight ratios of the two components; heating rate 5 °C/min.

WSN), respectively, values in close agreement with the heat of fusions reported in the previously mentioned studies.

In the presence of the oil medium, the DSC thermal curves of WSTSN and WSN samples were modified. As shown in **Figure 2**, with increasing oil content, the melting peaks of wood stanols (WSN) became broader, less symmetrical, and moved to lower temperatures. A similar melting behavior was reported for canola sediment (waxes) in oil (*19*, *22*) and for solid fats dispersed in liquid triglycerides (*23*, *24*). The broadening of the peak and the decline in T_m are attributed to some kind of solubility effect. In increased amounts of liquid phase, the solid fraction dissolved in it also increases at any given temperature, thereby resulting in broader endothermic transitions at lower temperatures. According to the solubility equation, the reciprocal of melting temperature of a solid is proportional to the logarithm of the molar fraction of the solid

$$\left(\frac{1}{T}-\frac{1}{T_0}\right)=-\frac{R}{\Delta \mathrm{H}}\ln x_2 \qquad (1)$$

where T and T_0 are the melting temperatures of the solid in solvent and in pure state, respectively, x_2 is the molar fraction of the solid (phytosterols), ΔH is the heat of fusion of the solid, and R is the universal gas constant. Although it is recognized that this equation applies to an ideal solution (single solute−solvent systems), its use has been previously adopted to treat melting data of heterogeneous blends such as waxes−canola oil mixtures (*19*) and milk-fats in oils (*25*), providing a description of melting temperature on the average molar fraction of the dissolved solids. Such a treatment provides a convenient empirical means to compare the melting behavior of binary oil−phytosterol systems of varying composition and origin. In this context, an average molecular weight of phytosterols was assumed to be 412 (M_w of sitosterol), while that of oil was around 880 based on a typical molecular structure of a triglyceride (fatty acid $C_{avg} = 18$). The melting temperatures of phytosterol−oil admixtures were taken as the peak temperature of their melting endotherms. **Figure 3** reveals linear relationships between the DSC melting temperature and the molar fraction of phytosterols in oil (estimated R^2 values were 0.96 and 0.93 for WSTSN− and WSN−oil mixtures, respectively) in fairly good agreement with eq 1. The heats of fusion (34.7 and 70.7 mJ/mg for WSTSN and WSN, respectively) calculated from the respective slopes are similar to the DSC

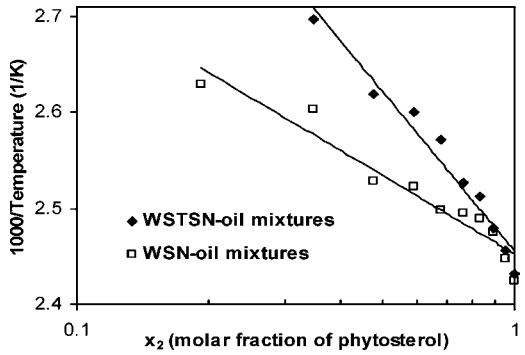

Figure 3. DSC melting temperatures of WSTSN and WSN as a function of molar fraction of phytosterol in oil according to eq 1.

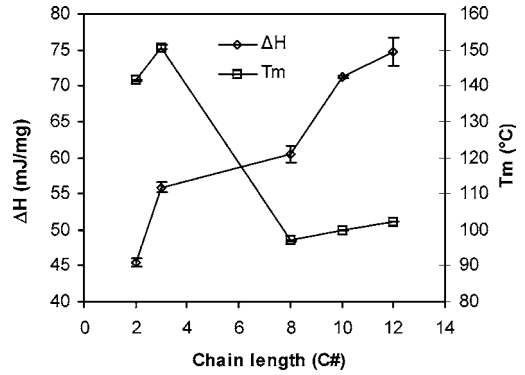

Figure 4. Peak melting temperature (°C) and fusion enthalpy of pure fatty acid esters of SSN as a function of the chain length of the acyl group.

experimental values (39.08 ± 1.74 mJ/mg for WSTSN and 74.9 ± 2.18 mJ/mg as the sum of the two endothermic transitions observed for WSN) determined for the phytosterol preparations alone.

Interesting observations on the DSC scans were also made for the fatty acid ester derivatives of SSN varying in the chain length of the acyl group (**Figure 4**). Among these derivatives, the acetate showed no major changes in T_m (141.5 ± 0.3 °C), whereas the propionate (f-3) was the only derivative, which exhibited a slightly higher melting temperature (150.8 ± 0.5 °C) than the free soy stanols. All other derivatives showed a substantial reduction in T_m (~ 40 °C), the most pronounced being for the capryloate (f-8) (i.e., esterification of phytostanols with midchain fatty acids (C8−C12) substantially suppressed their melting point). Generally, an increase of fusion enthalpy was observed with increasing chain length of the fatty acid moiety. According to Leeson and Flöter (*26*), the melting points and enthalpies of medium chain saturated β-sitosteryl esters (C6−C14) were among 346.9 and 360.3 K and 22.36−52.44 kJ/mol, respectively. Similar and even lower melting temperatures between 58.7 and 81.3 °C and heats of fusion in the range of 29.30−62.81 J/g have been reported for β-sitosteryl esters with MCFAs (C6−C12) produced by lipase catalyzed esterification reactions (*27*).

Solubility of Phytosterols in Corn Oil. The solubility of phytosterols in vegetable oils is an important issue from a food manufacturing point of view since the levels of added solutes may become an inhibiting factor for the stability of the final liquid formulation. **Figure 5** illustrates the dependence of solubilities of phytosterol samples as a function of temperature in the presence of corn oil. The determination of solubility was performed visually during the cooling step of corresponding phytosterol−oil liquid blends in a water bath under controlled

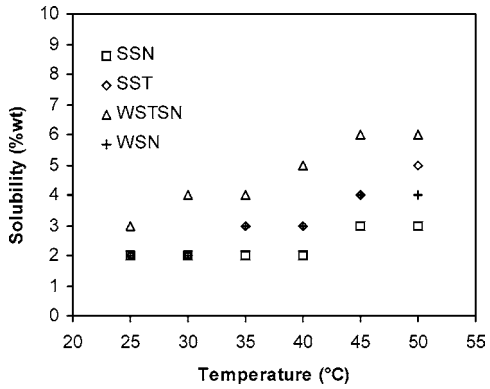

Figure 5. Solubility curves of phytosterol samples in corn oil as a function of temperature.

stirring and temperature as described previously. Agitation is frequently used to induce crystallization, with the most agitated solutions nucleating spontaneously at lower degrees of supercooling than quiescent ones. It is obvious that all phytosterol preparations were sparingly soluble in corn oil (2−3% at ambient temperature), whereas their solubility increased with the rise of temperature. However, differences in solubility were observed among the phytosterol preparations. Wood sterol−stanol (WSTSN) mixtures showed the highest solubility at all temperatures tested (presumably due to their heterogeneous composition), giving also the greatest solubility rise with the increase of temperature. This behavior was followed by soy sterols (SST), while corn oil containing soy stanols (SSN) crystallized, at concentration of 4 wt %, even at the highest observation temperature of 50 °C. Generally speaking, the solubility of samples containing only sterols or sterols in a higher ratio seems to be better dissolved in corn oil and thus the samples are more stable with respect to crystallization. Overall, the solubility of the sterol samples examined is reduced in the following order: WSTSN, SST, WSN, and SSN. Similar low solubility values, particularly at low temperatures, were also reported by Melñikov et al. (*3*) for sitosterol and sitostanol dissolved in sunflower and olive oils, as compared with the higher solubilities obtained when the same materials were solubilized in a more polar diglyceride-based oil and free oleic acid. The partial polar nature of phytosterols and phytostanols due to the presence of the hydrophilic OH group was claimed to be the reason for their increased solubilities in more polar solvents.

Crystallization Kinetics of Phytosterol−Oil Mixtures. A saturated solution is in thermodynamic equilibrium with the solid phase, at a specified temperature. It is possible, however, by cooling a hot concentrated solution slowly without agitation, to prepare solutions containing more dissolved solid than that represented by equilibrium saturation; such solutions are said to be supersaturated. The state of supersaturation is an essential requirement for all crystallization operations. A supersolubility curve represents temperatures and concentrations at which uncontrolled, spontaneous crystallization occurs (unstable or labile zone), whereas between solubility and supersolubility curves, there is a metastable zone (supersaturated region) where instant crystallization is improbable and nucleation is delayed for a period of time (*16*). This time lag for nucleation is called the induction time (τ) for crystallization and varies from a few minutes to many days depending on supersaturation, temperature, and external factors like stirring (*17*). Examples of liquid fat systems in a metastable state are oils that develop turbidity during storage. Therefore, the study of crystallization kinetics

of phytosterols in the metastable corn oil−sterol blends is of theoretical and practical interest. For this purpose, the transmittance at 600 nm of phytosterol−oil liquid blends at variable supersaturation levels as a function of time was measured isothermally. Typical transmittance−time curves of SSN−oil liquid preparations at different concentrations are given in **Figure 6**. The initial transmittance of a clear phytosterol−oil solution remains constant at the highest level (100%) for a period of time after which it decreases rapidly and finally levels off. The first period of constant transmittance indicated by the arrow (insert curve in **Figure 6**) corresponds to the induction time for nuclei formation, after which rapid growth and development of the crystals occurs, resulting in a deep decrease in transmittance. It is obvious that the more concentrated a solution is, the smaller the induction time for nucleation (**Figure 6**) is (i.e., induction time and nucleation rate are concentration or supersolubility dependent parameters).

As mentioned previously, the induction period can be affected by many external variables, so it cannot be regarded as a fundamental property of a system, nor can it be relied upon to yield basic information on the process of nucleation. Nevertheless, despite its complexity, the induction time has frequently been used as a measure of the nucleation event, making the simplifying assumption that it can be considered to be inversely proportional to the rate of nucleation, J ($\tau \propto J^{-1}$) (*16*). Liu et al. (*19*) used the following equation to describe the relationship between induction time and nucleation rate of waxes in canola oil:

$$\ln \tau = \text{constant} - \frac{\ln J}{4} \tag{2}$$

The rate of nucleation, J (e.g., the number of nuclei formed per unit time per unit volume) can be expressed in the form of the Arrhenius relationship commonly used for the rate of a thermally activated process (*16*)

$$J = A \exp\left(-\frac{\Delta G^*}{kT}\right) \tag{3}$$

where the pre-exponential coefficient A is a constant, k is the Boltzmann constant (1.38×10^{-23} J/K), T is the absolute temperature, and ΔG^* is the activation energy for nucleation. The activation energy ΔG^* can be calculated by the following equation (*16*):

$$\Delta G^* = \frac{16\pi\gamma^3\upsilon^2}{3k^2T^2(\ln S)^2} \tag{4}$$

where γ is the surface free energy between solid and liquid phases (J/m^2), υ is the molecular volume of the solid (m^3/molecule), and S is the supersaturation of the solution, defined by the ratio $S = C/C_s$ with C being the solution concentration and C_s the concentration at saturation. Expressing the supersaturation by the ratio S, however, conceals the possible effects of the absolute values of solute concentration. The average values of concentrations at saturation (C_s, % w/w) for all phytosterol samples examined (obtained by at least 6 replicates, as described previously) with their standard deviations (±SD) are presented in **Table 2**.

Substituting eqs 3 and 4 into eq 2, we obtain

$$\ln \tau = \text{constant} + \frac{4\pi\upsilon^2}{3k^3}\frac{\gamma^3}{T^3(\ln S)^2} \tag{5}$$

Hence, a plot of ln τ, corresponding to the different supersaturations imposed to the phytosterol−oil blends for a given temperature, versus $1/\ln^2 S$, should yield a straight line, the slope of which provides a value of the interfacial free energy, γ, since all parameters in eq 5 are either constants or can be measured. The experimental induction times as a function of the reciprocal of supersolubility of the phytosterol−oil mixtures (solutions) tested are illustrated in **Figure 7 a**,**b**. Linear regression analysis revealed good fits between induction times and $1/\ln^2 S$ for all samples tested (R^2 values shown in **Table 2**). A closer look at the regression lines reveals similar slopes (almost parallel lines) for the group of plant stanols (SSN and WSN) (**Figure 7a**) and superposition of the data sets for the plant stanol preparations (SST and WSTSN) (**Figure 7b**), implying that solid−liquid surface free energies between each group are alike but differentiate with respect to chemical nature of phytosterols (hydrogenated vs non-hydrogenated form) and/or initial compositional variation of the materials. Indeed, the highest γ value of 6.07 ± 0.06 mJ/m^2 was estimated for soy stanols followed by the wood stanols, whereas the calculated surface free energies for the plant sterol samples (**Table 2**) were smaller. A small interfacial free energy between a crystal and a solvent suggests a good affinity of the solvent for the solute or in other words a high solubility of the crystalline material (*17*). Thus, the mixed wood sterol stanol sample (WSTSN) exhibited the most stable solutions in corn oil among all the phytosterol preparations, followed by soy sterols, wood stanols, and soy stanols, in a

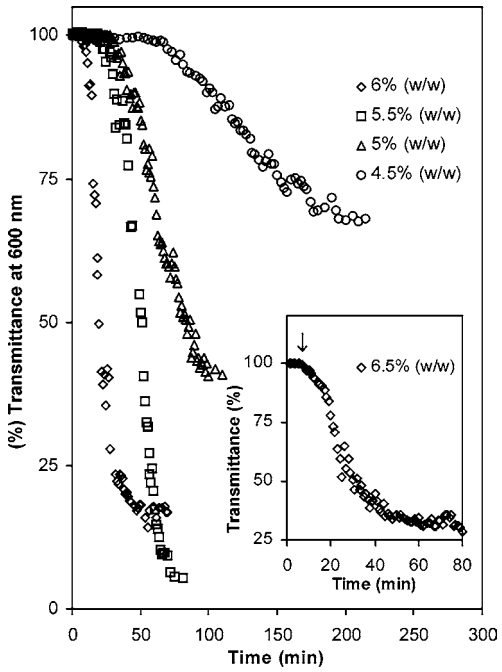

Figure 6. Transmittance–time curves of SSN–oil liquid blends at different solute concentrations as measured by spectrophotometry at 25 °C; the turbidity development of the SSN–oil blends after an induction time indicated by the arrow (inert transmittane–time curve).

Table 2. C_s, Slopes. and Estimated Surface Free Energies of Phytosterol Samples

sample	C_s[a] (% w/w) ± *SD*	slope[b] (*b*)	R^2	γ[c] (mJ/m^2) ± s_b
SSN	1.60 ± 0.22	1.462	0.99	6.07 ± 0.06
SST	2.57 ± 0.15	0.374	0.99	3.85 ± 0.01
WSTSN	3.22 ± 0.29	0.360	0.99	3.80 ± 0.01
WSN	1.76 ± 0.13	1.376	0.98	5.95 ± 0.10

[a] Average of six replications. [b] Slope of the regression lines shown in **Figure 7**. [c] Estimated by the slopes of regression lines according to eq 5.

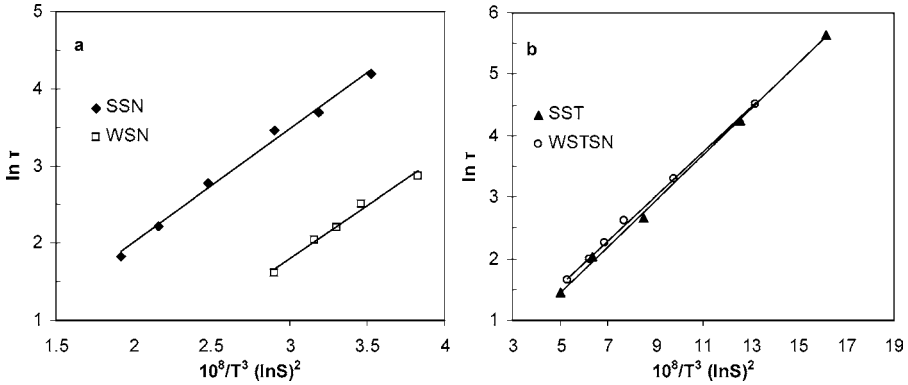

Figure 7. Induction time (τ) of crystallization at 25 °C as a function of supersaturation (S) of phytostanol (left) and phytosterol (right) solutions in corn oil.

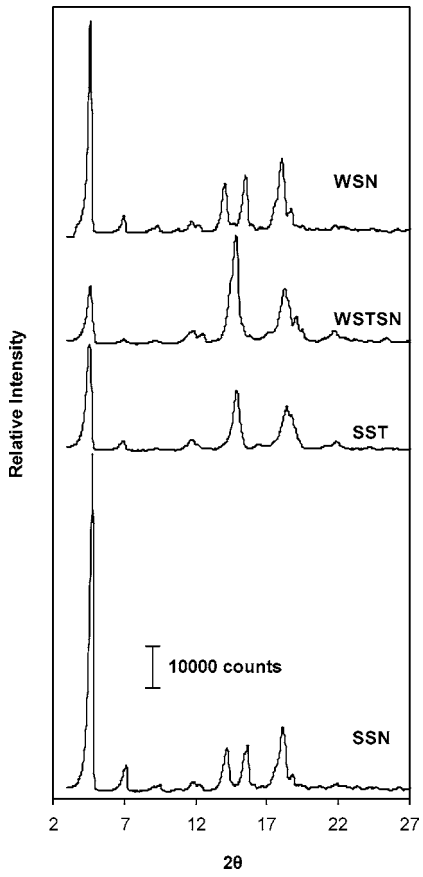

Figure 8. X-ray diffraction patterns of dehydrated commercial phytosterol samples.

decreasing order of stability. These results are in total agreement with the decreasing order of the experimental solubility data (**Figure 5**) and the values of the critical concentration at saturation, C_s (**Table 2**). The previously mentioned estimations for interfacial free energy between phytosterols and corn oil are comparable with the values of γ, calculated by the same method, for waxes isolated from canola oil, as reported by Liu et al. (*19*, *22*). The wax sediment−canola oil mixtures exhibited surface free energy values of 4.71 and 10.5 erg/cm^2 in the latter two studies, a variation that was attributed to the different degrees of supercooling of the materials used.

X-ray Patterns and Morphology of Phytosterol Preparations. The X-ray diffraction patterns of native phytosterol crystals are illustrated in **Figure 8**. It is clear that a similarity exists between XRD patterns of the materials with similar chemical composition (i.e., between sterols, SST, and WSTSN or between their hydrogenated products, stanols, SSN, and WSN), independent of plant origin (soy or wood). Thus, despite the fact that different extraction/isolation processes and plant sources may lead to variations in the composition of phytosterol preparations (relative amounts of the major phytosterols present in each mixture, **Table 1**), the diffraction angles and relative intensities of major peaks are similar within each group of the diffraction patterns. This finding is consistent with previous results of the XRD analysis of plant sterols derived either from wood pulp or vegetable oils that revealed similar profiles and crystallization behavior for both formulations (*3*). The diffraction peaks (2θ) for soy stanols (SSN) were observed at 2θ 4.8, 7.15, 9.55, 11.75, 12.25, 14.2, 15.65, 18.1, and 18.85°, while the respective diffraction angles for wood stanol (WSN) peaks were at positions 4.07, 7, 9.35, 11.75, 12.25, 14.1, 15.5, 18.05, and 18.7°. In contrast, the patterns of sterols differentiate slightly from those of stanols (i.e., diffraction peaks are shifted at lower or higher 2θ positions while others are absent). For soy sterols (SST), diffraction peaks appeared at 2θ 4.6, 6.9, 9.35, 11.7, 14.85, 16.5, 18.4, and 21.9° and for WSTSN at 2θ 4.6, 7, 9.15, 11.85, 12.5, 14.8, 18.25, 19.05, and 21.75°. Such variations in crystal structure between sterol and stanol samples can allow discrimination between phytosterol preparations of different composition and could account for the differences in solubility and surface free energy characteristics previously discussed. Generally, the XRD patterns of the commercial phytosterol−phytostanol samples presented in this work resemble closely those of anhydrous β-sitosterol (*13*, *21*) and β-sitosterol, sitostanol, and plant sterols from wood pulp and vegetable oils previously reported by Melñikov et al. (*3*).

A comparison between the XRD spectra of the crystalline commercial phytosterol preparations and the crystals obtained via recrystallization from corn oil revealed only small differences in the diffraction patterns, especially in terms of intensities of some peaks, but the general structural features were similar to their native counterparts (data not shown). With respect to the recrystallization process of phytosterols in oil, the X-ray findings of crystals obtained without or after agitation of the sterol−oil mixtures (liquid) also varied slightly, mainly on the relative intensities of the diffraction peaks. Such findings are in agreement with previous reports on sterols/stanols recrystallized in oil media (*3*). In the latter study, a lower resolution of the XRD spectra of phytosterol crystals obtained by crystallization from olive oil was attributed to the presence of trace amounts of amorphous material, contaminating the crystals that increased as background noise, as well as partially dissolved sterol/stanol crystals resulting in the reduction of peak sharpness. Small variations in crystallinity and resolution of the XRD spectra

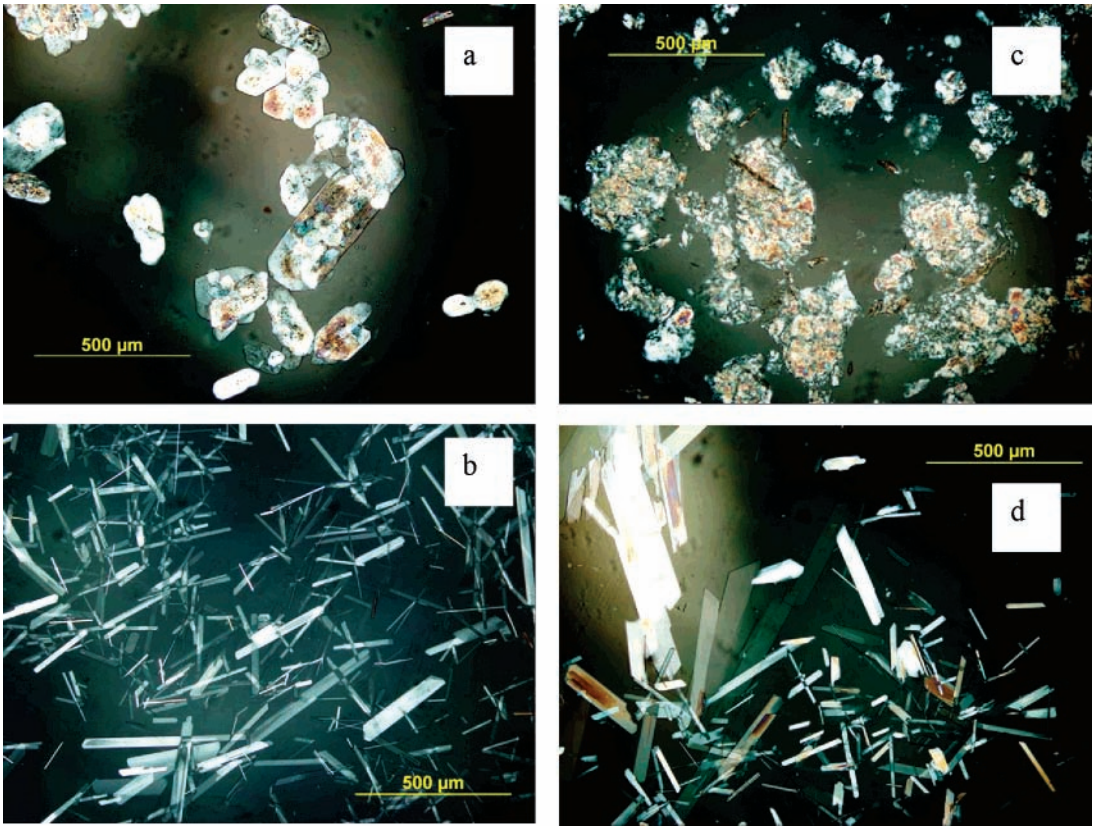

Figure 9. Micrographs of soy stanol (SSN, **a** and **b**) and wood sterol stanol (WSTSN, **c** and **d**) crystals suspended in oil; (**a** and **c**) native phytosterols and (**b** and **d**) crystals obtained after recrystallization of phytosterol–oil liquid blends (4% w/w at 25 °C) under gentle stirring.

were also observed in suspensions of β-sitosterol in medium chain triacylglycerol oil with increasing sterol concentration (*18*).

Differences in crystal morphology were further evaluated with optical microscopy. The size and crystal morphology could largely affect crystal aggregation phenomena and the rheological properties of oil−phytosterol blends and thereby influence the sensorial attributes of these systems. Representative micrographs of stanol and sterol crystals in the commercial and recrystallized preparations are given in **Figure 9**. In the native form, crystal aggregates exhibited plate-like morphologies, whereas wood stanols appeared as particles of smaller size lacking uniformity and mostly appearing as aggregated crystal clusters (**Figure 9a**,**c**). Crystal morphology was significantly altered after dissolution and recrystallization in the oil medium, particularly for recrystallized materials under mechanical shear (**Figure 9b**,**d**). In the latter preparations, thinner and smaller sized needle-like crystals were obtained after crystallization of both SSN and WSTSN preparations. In previous studies (*13*, *21*), crystal habits of β-sitosterol were lath shaped (anhydrous β-sitosterol) or needle-like (β-sitosterol monohydrate) when precipitated from dry acetone or acetone−water mixtures, respectively. Variations in crystal habit and size have been also reported by von Bonsdorff-Nikander et al. (*18*); phytosterol suspensions in oil exhibited plate-like crystals, which transformed to needle shaped, smaller in size crystallites with an increase in the concentration of β-sitosterol and/or the cooling rate of the suspensions.

Conclusion. Crystalline samples of soy and wood sterols or stanols examined in this study had high melting points (138−145 °C), whereas their phytosterol corn oil blends exhibited melting peaks at lower temperatures, following the typical solubility law of a solute−solvent (diluent) mixture. Moreover, suppression of the melting point was found for the fatty acid esters of soy stanols, especially when the stanols were esterified with midchain fatty acyl groups (C8−C12). Plant sterols and stanols tested were sparingly soluble in corn oil (2−3% at ambient temperature) and therefore prone to crystallization in the oil medium after an induction period at concentrations slightly above this range. Solubility curves and crystallization kinetics revealed differences in phase transition behavior between sterol and stanol preparations examined, irrelevant to the plant origin of these materials. In general, plant sterols were more soluble and gave more stable sterol−oil liquid blends than the respective stanol preparations, as evidenced by the critical concentration at saturation and the surface free energy values determined. Differences were also observed in the crystal structure and morphology of the commercial phytosterol preparations, as well as among crystalline samples regained after crystallization in oil. In conclusion, the crystallinity of phytosterols and their low solubility in edible oils constitute limiting factors for their incorporation into food matrices. The inclusion of phytosterols as functional ingredients in oil-based delivery systems requires further investigation to obtain stable formulations (e.g., with the aid of emulsifiers) that would permit a much greater concentration of soluble material from these bioactives.

ACKNOWLEDGMENT

The authors thank Prof. N. Barbayannis (Dept. of Soil Science, Faculty of Agriculture) for conducting the XRD measurements.

LITERATURE CITED

(1) Katan, M. B.; Grundy, S. M.; Jones, P.; Law, M.; Miettinen, T.; Paoletti, R. Efficacy and safety of plant stanols and sterols in the management of blood cholesterol levels. *Mayo Clinic Proc.* **2003**, *78*, 965−978.

(2) Ostlund, R. E., Jr. Phytosterols in human nutrition. *Annu. Rev. Nutr.* **2002**, *22*, 533−549.
(3) Melñikov, S. M. M.; Seijen ten Hoorn, J. W.; Bertrand, B. Can cholesterol absorption be reduced by phytosterols and phytostanols via a cocrystallization mechanism? *Chem. Phys. Lipids* **2004**, *127*, 15−33.
(4) Tapiero, H. D.; Townsend, M.; Tew, K. D. Phytosterols in the prevention of human pathologies. *Biomed. Pharmacother.* **2003**, *54*, 321−325.
(5) Salen, G.; Shefer, S.; Nguyen, L.; Ness, G. C.; Tint, G. S.; Shore, V. Sitosterolemia. *J. Lipid Res.* **1992**, *33*, 945−955.
(6) Heinemann, T.; Axtmann, G.; von Bergmann, K. Comparison of intestinal absorption of cholesterol with different plant sterols in man. *Eur. J. Clin. Invest.* **1993**, *23*, 827−831.
(7) Lütjohann, D.; Björkhem, I.; Beil, U. F.; von Bergmann, K. Sterol absorption and sterol balance in phytosterolemia evaluated by deuterium-labeled sterols: effect of sitostanol treatment. *J. Lipid Res.* **1995**, *36*, 1763−1773.
(8) Czubayko, F.; Beumers, B.; Lammsfuss, S.; Lütjohann, D.; von Bergmann, K. A simplified micro-method for quantification of fecal excretion of neutral and acidic sterols for outpatient studies in humans. *J. Lipid Res.* **1991**, *32*, 1861−1867.
(9) Quilez, J.; Garcia-Lordam, P.; Salas-Salvado, J. Potential uses and benefits of phytosterols in diet: present situation and future directions. *Clin. Nutr.* **2003**, *22*, 343−351.
(10) Ling, W. H.; Jones, P. J. H. Mini review dietary phytosterols: a review of metabolism, benefits, and side effects. *Life Sci.* **1995**, *57*, 195−206.
(11) Moghadasian, M. H.; Frohlich, J. J. Effects of dietary phytosterols on cholesterol metabolism and atherosclerosis: clinical and experimental evidence. *Am. J. Med.* **1999**, *107*, 588−594.
(12) Salo, P.; Wester, I. Low-fat formulations of plant stanols and sterols. *Am. J. Cardiol.* **2005**, *96*, 51−54.
(13) Christiansen, L. I.; Rantanen, J. T.; von Bonsdorff, A. K.; Karjalainen, M. A. A novel method of producing a microcrystalline β-sitosteryl suspension in oil. *Eur. J. Pharm. Sci.* **2002**, *15*, 261−269.
(14) Christiansen, L. I.; Lähteenmäki, P. L. A.; Mannelin, M. R.; Seppänen-Laakso, T. E.; Hiltunen, R. V. K.; Yliruusi, J. K. Cholesterol-lowering effect of spreads enriched with microcrystalline plant sterols in hypercholesterolaemic subjects. *Eur. J. Nutr.* **2001**, *46*, 66−73.
(15) Jones, P. J. H.; MacDougal, D. E.; Ntanios, F.; Vanstone, C. A. Dietary phytosterol as cholesterol-lowering agents in humans. *Can. J. Physiol. Pharmacol.* **1997**, *75*, 217−227.
(16) Mullin, J. W. Solutions and solubility, Nucleation. In *Crystallization*, 3rd ed.; Butterworth-Heinemann Ltd.: Oxford, 1993; pp 81−127, 172−201.
(17) Boistelle, R. Fundamentals of nucleation and crystal growth. In *Crystallization and Polymorphism of Fats and Fatty Acids*; Garti, N., Sato, K., Eds.; Marcel Dekker, Inc.: New York, 1988; pp 189−226.
(18) von Bonsdorff-Nikander, A.; Karjalainen, M.; Rantanen, J.; Christiansen, L.; Yliruusi, J. Physical stability of amicrocrystalline β-sitosterol suspension in oil. *Eur. J. Pharm. Sci.* **2003**, *19*, 173−179.
(19) Liu, H.; Biliaderis, C. G.; Przybylski, R.; Eskin, N. A. M. Phase transitions of canola oil sediment. *J. Am. Oil Chem. Soc.* **1993**, *70*, 441−448.
(20) Narayana Kalkura, S.; Devanarayanan, S. Growth of β-sitosterol crystals in silica gel and their characterization. *J. Mater Sci. Lett.* **1989**, *8*, 481−482.
(21) Christiansen, L.; Karjalainen, M.; Seppänen-Laakso, T.; Hiltunen, R.; Yliruusi, J. Effect of β-sitosterol on precipitation of cholesterol from non-aqueous and aqueous solutions. Int. J. Pharm. **2003**, *254*, 155−166.
(22) Liu, H.; Biliaderis, C. G.; Przybylski, R.; Eskin, N. A. M. Physical behavior and composition of low- and high-melting fractions of sediment in canola oil. *Food Chem.* **1995**, *53*, 35−41.
(23) Norton, I. T.; Lee-Tuffnell, C. D.; Ablett, S.; Bociek, S. M. A calorimetric, NMR, and X-ray diffraction study of the melting behavior of tripalmitin and tristearin and their mixing behavior with triolein. *J. Am. Oil Chem. Soc.* **1985**, *62*, 1237−1244.
(24) Hale, J. E.; Schroeder, F. Phase behavior of triolein and tripalmitin detected by differential scanning calorimetry. *Lipids* **1981**, *16*, 805−809.
(25) Timms, R. E. Solubility of milk-fat, fully hardened milk-fat, and milk-fat hard fraction in liquid oils. *Aust. J. Dairy Technol.* **1978**, *33* (4), 130−135.
(26) Leeson, P.; Flöter, E. Solidification behavior of binary sitosteryl ester mixtures. Food Res. Int. **2002**, *35*, 983−991.
(27) Vu, P.-L.; Shin, J.-A.; Lim, C.-H.; Lee, K.-T. Lipase catalyzed production of phytosteryl esters and their crystallization behavior in corn oil. *Food Res. Int.* **2004**, *37*, 175−180.

Received for review August 23, 2006. Revised manuscript received December 17, 2006. Accepted January 5, 2007. This work was carried out under the financial support of the Greek State Scholarships Foundation (IKY) (scholarship granted to H.V.).

JF0624289